Primary Electronic Thermometry Using the Shot Noise of a Tunnel Junction

Lafe Spietz,[1]* K. W. Lehnert,[1,2] I. Siddiqi,[1] R. J. Schoelkopf[1]

We present a thermometer based on the electrical noise from a tunnel junction. In this thermometer, temperature is related to the voltage across the junction by a relative noise measurement with only the use of the electron charge, Boltzmann's constant, and assumption that electrons in a metal obey Fermi-Dirac statistics. We demonstrate proof-of-concept operation of this primary thermometer over four orders of magnitude in temperature, with as high as 0.1% accuracy and 0.02% precision in the range near 1 kelvin. The self-calibrating nature of this sensor allows for a much faster and simpler measurement than traditional Johnson noise thermometry, making it potentially attractive for metrology and for general use in cryogenic systems.

Temperature is an important quantity in every field of science and technology. Although a vast selection of thermometers exists, there is no simple thermometry solution for all applications. Ideally, a thermometer should be fast, compact, accurate, independent of other system variables such as magnetic field, and simple to use. It is desirable for a thermometer to be primary, that is, to relate temperature to other measurable quantities through a known physical law. This eliminates the need for initial calibration and the possibility of calibration drift in the sensor. Almost all of the thermometers in use outside of standards labs today are secondary, meaning they need to be calibrated by referencing to some primary thermometer. We introduce a primary electronic thermometer that is fast and compact, operates over four decades in temperature, and relates temperature to voltage with the use of well-understood physics.

Several primary thermometers presently exist (1), but these are of limited practical use for various reasons. The classic example of a primary thermometer is the constant-volume gas thermometer (CVGT). The CVGT relates temperature (T) to the pressure of a gas with the use of the ideal gas law $PV = Nk_BT$, where P, V, N, and k_B are the pressure, volume, number of particles, and Boltzmann constant, respectively. The CVGT and several other gas thermometers (2) rely on the behavior predicted by Maxwell-Boltzmann statistics and have been used for thermometry for more than a century (3). The Planck and Stefan-Boltzmann radiation laws extend primary thermometry up to the highest temperatures measured. These laws follow from the treatment of a bath of photons as an ideal Bose gas. The shot noise thermometer (SNT) uses the voltage-dependent electrical noise from a tunnel junction to relate temperature to voltage with the use of only the ratio e/k_B. The form of this signal, called the junction noise, follows directly from the fact that electrons in a metal obey Fermi-Dirac statistics and from some basic assumptions about the tunnel barrier. There is a desire in metrology to establish quantum standards such as the Josephson volt and the quantum Hall resistance (4), which relate a unit to other units in the International System of Units with the use of well-understood quantum physics. The SNT could eventually serve as such a standard by relating temperature to voltage, which can be more easily measured to high accuracy.

We measured the junction noise and demonstrated its use for thermometry from room temperature down to the base temperature of a dilution refrigerator. We verified the functional form of the noise to 200 parts per million (ppm) with temperature as a fit parameter. We demonstrated the operation of the SNT with accuracy as good as a part in 10^3 in the range of a few kelvin and as good as 200 ppm precision at 0.5 K. The temperatures as measured by the SNT agree with our available secondary thermometers to within their stated calibration accuracy from 50 mK to about 25 K.

The SNT shares many of the advantages and some common aspects with the earlier Coulomb blockade thermometer (CBT) (5–9), which has been extensively studied and developed into a commercial product. Both use electron tunneling in a junction to relate temperature to voltage without requiring external calibrations. The Coulomb blockade device, however, uses the nonlinearity in the electrical conductance due to electron-electron interactions and requires high-resistance, ultrasmall junctions, which presently limits the range for a single sensor to about two orders of magnitude in temperature and the maximum temperature of primary operation to about 20 K. The SNT uses instead the simpler physics of shot noise in large junctions, allowing a single sensor to operate over a substantially wider range and with a factor of five greater absolute accuracy (0.1%) as compared to the present state (0.5%) of Coulomb blockade devices (8). The CBT has also been shown to be independent of magnetic field up to ~ 30 T (9). The high-magnetic-field performance of the CBT is a strong indication that the SNT will also be field-independent.

The first technique for primary electronic thermometry relies on a measurement of the Johnson-Nyquist noise, or thermal equilibrium noise, of a resistor and has been used for decades (10), although it is of limited practical use. In 1928, Nyquist derived and Johnson measured the formula $S_I = 4k_BT/R$, where S_I is the current spectral density and R is the resistance, for the current spectral density (in $\frac{A^2}{Hz}$) of the noise (11–13). Because resistance is an easy quantity to measure accurately, the challenge of Johnson noise thermometry is to obtain an accurate measurement of the noise power generated by the resistor. This is extremely difficult: The signals involved are very small, particularly at low temperatures, and high-gain amplifiers must be used. The gain and bandwidth of the entire measurement chain must therefore be known to the desired accuracy of the ultimate temperature determination. In order to have an acceptable level of uncertainty in the gain as a function of frequency, the bandwidths of noise thermometry experiments are typically limited to the kHz range. The Dicke radiometer formula, $\delta T/T = 1/\sqrt{B\tau}$, gives the fractional error for a noise measurement, where B is the bandwidth and τ is the measurement time (14, 15). For a bandwidth of 100 kHz, the time required to do a measurement with 1 mK accuracy with a system noise temperature of 5 K is several minutes, too slow for everyday use. Because of the complexity and long integration times involved, typically only temperature metrologists and those concerned with the study of noise have used Johnson noise to measure temperature (10, 16).

Over the years, however, several experimental techniques have been developed to overcome the limitations of traditional noise thermometry. Use of superconducting quantum interference device (SQUID) amplifiers has led to noise temperatures as low as 30 mK, greatly increasing the speed of measurements at the very lowest temperatures (17). Another important innovation in noise thermometry is the relation of noise power from the sensor resistor to frequency with the use of the resistively shunted SQUID (R-SQUID), overcoming the need for very high accuracy knowledge of am-

[1]Department of Applied Physics, Department of Physics, Yale University, New Haven, CT 06520, USA. [2]JILA, National Institute of Standards and Technology and University of Colorado, Boulder, CO 80309, USA.

*To whom correspondence should be addressed. E-mail: lafe.spietz@yale.edu

plifier gains (*18*, *19*). A promising noise thermometer based on the ac Josephson standard is being investigated by a collaboration of several standards labs (*20*). This thermometer shares with the SNT the prospect of relating temperature to the Josephson voltage standard.

Although not of direct interest for most noise thermometry experiments, another important type of electrical noise is shot noise, first described by Schottky in 1918 (*21*). Shot noise appears in any system in which current consists of random discrete tunneling events, such as a tunnel junction or a vacuum tube. Shot noise is both frequency- and temperature-independent and has the current spectral density $S_I = 2eI$, where I is current. The junction noise used for the SNT displays both shot noise and Johnson noise, with a voltage-dependent transition between the two regimes. This temperature-dependent transition voltage allows us to determine temperature with only the use of a measurement of the dc voltage and a relative noise power measurement.

A tunnel junction can be modelled as a pair of ideal Fermi reservoirs separated by a tall, thin energy barrier. The tunneling rate from a given energy level in one metal into the other metal can be evaluated by Fermi's golden rule. It is well known that the tunneling rates are given by

$$\Gamma_{r\to l(l\to r)} = \frac{2\pi}{\hbar} \int |\langle l|M(E)|r\rangle|^2 D^2(E)$$

$$f_{r(l)}(E)[1 - f_{l(r)}(E)]dE \quad (1)$$

where $\langle l|M(E)|r\rangle$ is the tunneling matrix element from the left to the right side of the junction, $D(E)$ is the density of states, and $f_l(E)$ and $f_r(E) = f_l(E - eV)$ are Fermi functions used to count the empty and filled states on the left and right reservoirs, respectively (*22*). For a sufficiently tall, thin barrier, the tunneling amplitude and the density of states near the Fermi energy can be considered to be independent of energy. The occupation probability of any given state in one of the metals is given by a Fermi function. Thus, under the conditions that $[eV_{bias}, k_BT] \ll E_{barrier}$, all the terms can be moved outside of the integral except the Fermi functions. The current through the junction can be found by taking the difference of these two rates to get

$$I = I_r - I_l = \frac{2\pi e}{\hbar} |\langle l|M(E_F)|r\rangle|^2$$

$$D(E_F)^2 \int [f_r(E) - f_l(E)]\, dE = V/R \quad (2)$$

In other words, under these conditions, the junction is just an ohmic resistor with no temperature dependence. To find the current spectral density of the noise, we just evaluate the sum of the rates across the barrier instead of the difference. Evaluation of the integral gives the well-known result (*23–25*)

$$S_I(V) = \frac{2}{R} \int \{f_r(E)[1 - f_l(E)] + f_l(E)[1 - f_r(E)]\}$$

$$dE = \frac{2eV}{R} \coth\left(\frac{eV}{2k_BT}\right) = 2eI \coth\left(\frac{eV}{2k_BT}\right)$$

$$(3)$$

Unlike the current, this expression has a temperature-dependent scale that follows directly from the Fermi-Dirac distribution. Evaluation of Eq. 3 at zero bias voltage yields the Johnson result $S_I = 4k_BT/R$, as required by the fluctuation-dissipation theorem (*26*), whereas in the limit $eV \gg k_BT$ Eq. 3 reduces to $S_I = 2eI$, or shot noise (Fig. 1). As a function of voltage, the junction noise changes smoothly from Johnson noise to shot noise in a way that depends only on k_B, e, and a simple analytic function. Thus, the voltage dependence of the noise in Eq. 3 is analogous to the equation of state of the ideal gas.

By measuring the noise as a function of voltage, the temperature can be determined from the voltage scaling of this transition independent of the gain or noise of the amplifier chain and detector. This frees us from the major limitations of traditional noise thermometry: the need to calibrate gain, noise temperature, and bandwidth to high accuracy. The elimination of the need for absolute accuracy in the amplifier chain calibrations allows much more freedom in the selection of components. In particular, we may replace the kHz bandwidth amplifier typically used by microwave amplifiers with hundreds of MHz of bandwidth, allowing for a much faster readout. In general, our amplifier has a frequency-dependent gain $g(\omega)$ and a noise temperature $t_n(\omega)$, and we can fit the total noise power P to the equation

$$P(V,T) = \int d\omega g(\omega) \left[t_n(\omega) + \right.$$

$$\left. \frac{eV}{2k_B} \coth\left(\frac{eV}{2k_BT}\right) \right] =$$

$$G\left[T_n + \frac{eV}{2k_B} \coth\left(\frac{eV}{2K_BT}\right) \right] \quad (4)$$

with average gain-bandwidth product G, average noise temperature T_n, and temperature T as fit parameters. Equation 4 shows (Fig. 1) that the SNT relates temperature to voltage in a way that is independent of G and T_n. The method is also independent of effects such as frequency-dependent gain or impedance of the sensor, the transmission of the tunnel barrier, the sensor resistance, or any other effect that does not vary with DC bias voltage (*27*). Thus, our method retains the advantages of noise thermometry, being primary and electronic, but is much faster and simpler.

For a sensor, we used an Al-AlO$_x$-Al tunnel junction, fabricated with the use of electron

beam lithography and the Dolan bridge double-angle evaporation technique (*28*, *29*). We designed the junctions to be about 50 ohms to match to the impedance of the microwave electronics. These junctions show similar conductance characteristics to devices from published literature (*30*), which have a barrier height of about 2 V and a barrier thickness of about 1 nm. During all measurements below 1.5 K, we applied a 0.5-T magnetic field to keep the aluminum in a nonsuperconducting state, although the need for this field could be eliminated by using a normal metal or by adding a local permanent magnet.

In order to verify the form of the junction noise, we simultaneously measured the dc voltage and the radio frequency (rf) noise power (Fig. 2). We varied the bias across the device to measure the noise as a function of voltage across the junction. By fitting these data to the predicted junction noise with a least squares fit, we can determine a temperature T_{SNT}. We measured the junction noise as a function of temperature from 0.260 to 300 K in a variable-temperature ^{3}He refrigerator and from 0.01 through 4.2 K with the use of a dilution refrigerator.

Before the SNT can be trusted as a thermometer, we must verify the validity of our "ideal gas law," that is, whether the junction noise follows the prediction of Eq. 3. To do this, we display the noise data in a dimensionless form, normalizing the noise power relative to the zero bias noise and the voltage relative to the temperature (Fig. 3). The data at all temperatures agree well with a simple universal form over four decades in temperature.

The largest deviations of the noise from the expected form occur at the highest and lowest temperatures. At temperatures above about 30 K, we see deviations in the functional form by as much as a few percent. Because the devices are fabricated on a half-micrometer-thick layer of silicon dioxide
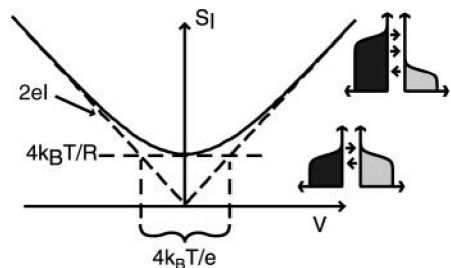

Fig. 1. Theoretical plot of current spectral density of a tunnel junction (Eq. 3) as a function of dc bias voltage. The diagonal dashed lines indicate the shot noise limit, and the horizontal dashed line indicates the Johnson noise limit. The voltage span of the intersection of these limits is $4k_BT/e$ and is indicated by vertical dashed lines. The bottom inset depicts the occupancies of the states in the electrodes in the equilibrium case, and the top inset depicts the out-of-equilibrium case where $eV \gg k_BT$.

atop a silicon wafer, which conducts at temperatures above about 30 K, there is an ac current path around the junction, which should depend on the bias voltage. This voltage-dependent attenuation of the rf signal would cause voltage-dependence of the noise temperature, leading to anomalous readings. If this explanation proves to be correct, this could be eliminated by fabricating the junctions on a totally insulating substrate such as quartz or sapphire. At 10 mK, $k_B T/e$ is less than 1 μV, so to measure temperature accurately the dc bias must be stable to better than 1 μV. At the lowest temperatures, we observe an ~40 Hz microphonic signal on the bias of about 1 μV in amplitude, which leads to an increase in the apparent T_{SNT}.

To test the accuracy of the SNT over a wide range, we compared the T_{SNT} to those of a calibrated rhodium-iron resistance thermometer above 1.6 K and a calibrated ruthenium oxide resistance thermometer below 4 K (31). The temperature determined with the SNT is compared against these secondary thermometers in Fig. 4. In the range from 25 mK to 25 K, the dominant error is the calibration uncertainty of the secondary thermometers used for comparison, whereas the highest and lowest ranges display notable deviations of apparent temperature because of the mechanisms described above. This comparison highlights the wide temperature range of the SNT, because several conventional thermometers were required to cover the whole range.

To low-temperature physicists, the most important temperature range for thermometry is also the most difficult: below 1 K. In this range, resistive thermometers are particularly unsatisfactory, with the best ruthenium oxide sensors having a 10% calibration uncertainty at 50 mK and no calibrations available below
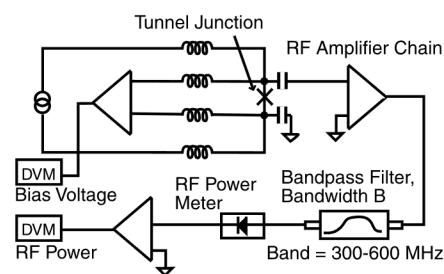
50 mK. Several exotic thermometers in this temperature range exist, such as nuclear orientation thermometry and the ^{3}He melting curve, which are too complex or expensive for general use. The CBT (5–9) is a primary thermometer in this range that has been commercialized for general use. The SNT provides another thermometry solution that is competitive with the CBT in this range, but which extends over a wider range and for which electron-phonon decoupling (32) is likely to be less severe because electron diffusion can enhance the cooling due to the single-junction geometry. The SNT can provide high-accuracy, fast, primary thermometry from room temperature to the base temperature of a dilution refrigerator.

To test the ultimate precision of the SNT, we regulated the temperature at close to 0.5 K, with temperature maintained to 200 ppm. By increasing the integration time per point, we were able to measure temperature with a precision of 200 ppm as well as to verify the agreement of the noise to the theory to 200 ppm. The precision improves with time τ close to the ideal behavior $1/\sqrt{\tau}$. Relative microwave noise measurements at the ppm level are routine in cosmic microwave background studies (33), which demonstrates that the ultimate precision of the SNT will not be limited by the statistical uncertainty of the microwave noise measurement.
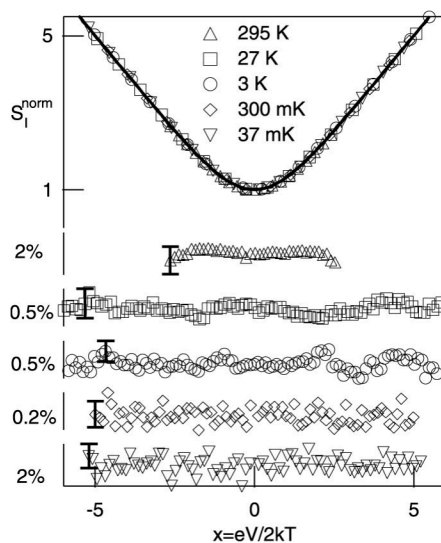
Although this test at 0.5 K revealed no deviations from the ideal junction noise law, there are several systematic effects that should appear at higher precision and at the lowest and highest temperatures. Deviations from linearity of the rf power amplifiers and the square law detector lead to deviations of the measured noise curve from the theory. These errors can be kept at the part-in-a-thousand level easily by attenuating the signal into the linear range of the detector and can be calibrated out by comparing curves taken with different attenuations. They could also be eliminated by a null-balancing noise measurement (34), which adds the noise of two separately biased junctions. By this method, the noise power could be limited to a range over which the rf chain is linear to a part per million. One type of systematic effect that deserves mention but that we have not observed at the present level of precision is self-heating. By applying a bias to the junction, we are injecting heat into the system. However, our calculations show that the heating should be at the level of tens of ppm and could be reduced to the ppm level with better design of leads for optimal cooling (35).

Another potential systematic error comes from any kind of nonlinearity in the current-voltage characteristic of the junction. We believe that we have not yet observed this as a dominant systematic effect, although we hope to be able to correct for it with the use
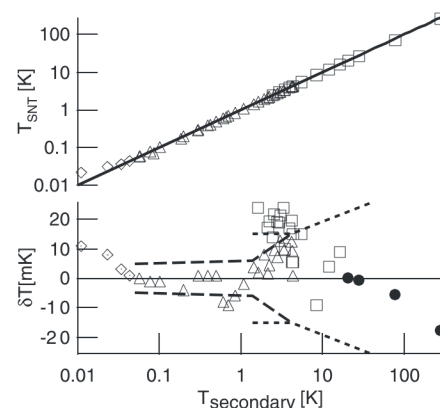

Fig. 2. Apparatus used for measurement of junction noise. Inductively coupled leads block high frequencies and allow the junction to be current-biased with one pair of leads, whereas the voltage is measured with the other pair of leads. Capacitively coupled leads allow the noise to be measured simultaneously. The noise signal is amplified by a cryogenic high electron mobility transistor amplifier and a chain of rf amplifiers, which provide about 70 dB of gain and a noise temperature of 10 K. The output of this chain is measured by a Schottky diode, which converts noise power to a dc voltage. Voltages are read out on digital volt meters (DVMs).

Fig. 3. Normalized junction noise plotted versus normalized voltage at various temperatures. Noise power is normalized to the zero bias (Johnson) noise, and bias voltage is scaled relative to temperature. In these units, the data follow the universal function $x\coth(x)$, depicted by the solid line. The residuals have the indicated fractional standard deviations and are shown below. This plot shows that the "gas law" for the junction noise is obeyed over four decades in temperature, with a significant systematic effect at the room temperature. Error bars indicate stated approximate SD of residuals.

Fig. 4. Comparison of temperature as measured by the SNT (T_{SNT}) to temperature as measured by secondary thermometers ($T_{secondary}$). Temperature is displayed on logarithmic axes, and the solid line indicates the line $T_{SNT} = T_{secondary}$. The bottom plot depicts deviations between the temperatures. Diamonds represent comparison with an Oxford Instruments (Witney, UK) ruthenium oxide thermometer; triangles, comparison with the Lakeshore Cryotronics ruthenium oxide thermometer; squares, comparison with a rhodium-iron thermometer (31); and circles, the deviation from the rhodium iron divided by 1000 (they represent temperatures in K, not mK). The dashed and dotted lines indicate the stated calibration uncertainties in the secondary thermometers.

of the measured nonlinearity of the current in the junction to adjust the theoretical noise curve. This effect increases with bias voltage and so becomes more important at higher temperatures. Systematic effects at the lowest temperatures include nonlinearities in the conductance because of Coulomb blockade effects (36) and the frequency dependence of the noise at temperatures for which hf is comparable to k_BT, where f is the measurement frequency and h is Planck's constant. This quantum correction to the noise was observed (37) in a mesoscopic gold wire and can be easily corrected with a modification of the noise formula or eliminated by reducing the frequency of the measurement.

The above discussions address the precision of the SNT, but not the accuracy. To achieve the 1 to 100 ppm accuracy required to be of metrological interest, the linearity of the rf chain, the accuracy of the bias voltage measurement, and the precision of the temperature must all be at that accuracy, and the deviations in the noise from our simple model must be accounted for to that accuracy. The linearity of the measurement can be addressed by use of a null-balancing noise measurement as mentioned above, and part-per-million voltage accuracy can be achieved by using a well-calibrated nanovoltmeter. The nonlinearities in the noise from the junction should be correctable with the use of the measured voltage dependence of the conductance. If the accuracy can be brought down to the part-per-million level at the triple point of water, it may be possible to determine Boltzmann's constant directly (38). Even a 10 ppm accuracy measurement admits the possibility of determining the thermodynamic uncertainty of the low end of ITS-90 (40) and the high end of PLTS-2000 to competitive accuracy. Because the SNT has the desirable properties of being fast, compact, easy to use, and accurate over a wide range, it may have a much broader field of application than present primary thermometers.

References and Notes
1. R. L. Rusby et al., Metrologia **33**, 409 (1996).
2. M. R. Moldover et al., Phys. Rev. Lett. **60**, 249 (1988).
3. H. L. Callendar, Philos. Mag. **48**, 519 (1899).
4. B. N. Taylor, T. J. Witt, Metrologia **26**, 47 (1989).
5. J. P. Pekola, K. P. Hirvi, J. P. Kauppinen, M. A. Paalanen, Phys. Rev. Lett. **73**, 2903 (1994).
6. J. P. Kauppinen, K. T. Loberg, A. J. Manninen, J. P. Pekola, Rev. Sci. Instr. **69**, 4166 (1998).
7. P. Delsing et al., Physica B **194**, 27 (1994).
8. A. J. Manninen et al., Physica B **284–288**, 2010 (2000).
9. J. P. Pekola et al., J. Low Temp. Phys. **128**, 263 (2002).
10. D. R. White et al., Metrologia **33**, 325 (1996).
11. J. B. Johnson, Nature **119**, 50 (1927).
12. J. B. Johnson, Phys. Rev. **32**, 97 (1928).
13. H. Nyquist, Phys. Rev. **32**, 110 (1928).
14. D. R. White, E. Zimmermann, Metrologia **37**, 11 (2000).
15. R. H. Dicke, Rev. Sci. Instrum. **17**, 268 (1946).
16. R. A. Webb, R. P. Giffard, J. C. Wheatley, J. Low Temp. Phys. **13**, 383 (1973).
17. C. P. Lusher et al., Meas. Sci. Technol. **12**, 1 (2001).
18. R. A. Kamper, J. E. Zimmerman J. Appl. Phys. **42**, 132 (1971).
19. R. J. Soulen Jr., W. E. Fogle, J. J. Colwell, J. Low Temp. Phys. **94**, 385 (1994).
20. S. P. Benz, J. M. Martinis, S. W. Nam, W. L. Tew, D. R. White, in the Proceedings of Tempmeko 2001 (www.cstl.nist.gov/div836/836.05/papers/Tempmeko_01_JNT.pdf).
21. W. Schottky, Ann. Phys. **57**, 541 (1918).
22. T. Van Duzer, C. W. Turner, Principles of Superconductive Devices and Circuits (Elsevier North Holland, New York, 1981), pp. 75–78.
23. R. A. Pucel, Proc. IRE **49**, 1080 (correspondence) (1961).
24. A. J. Dahm et al., Phys. Rev. Lett. **22**, 1416 (1969).
25. D. Rogovin, D. J. Scalpino, Ann. Phys. **86**, 1 (1974).
26. H. B. Callen, T. A. Welton, Phys. Rev. **83**, 34 (1951).
27. For example, even in a diffusive metal wire where the shot noise has the sub-Poisson value $S_1 = 2eI/3$ (37), the temperature extracted is the same.
28. J. Niemeyer, PTB-Mitt. **84**, 251 (1974).
29. G. J. Dolan, Appl. Phys. Lett. **31**, 337 (1977).
30. S. K. Tolpygo et al., IEEE Trans. Appl. Supercond., in press.
31. We used a rhodium-iron resistance thermometer (RF800-4-1.4L, Lakeshore Cryotronics, Westerville, OH, www.lakeshore.com) and a ruthenium-oxide resistance thermometer (RX202A-AA, Lakeshore Cryotronics).
32. J. P. Kauppinen, J. Pekola, Phys. Rev. B **54**, R8353 (1996).
33. L. Page, D. Wilkinson, Rev. Mod. Phys. **71**, S173 (1999).
34. J. D. Kraus Radio Astronomy (Cygnus-Quasar Books, Powell, OH, 1986), pp. 7–16.
35. At low temperatures, we assume diffusion cooling and use the Wiedemann-Franz law to compute the heating due to the finite lead resistance. Because the thermal conductance is proportional to temperature and the maximum power dissipated scales with temperature squared, the fractional temperature error is constant with temperature.
36. J. P. Kauppinen, J. P. Pekola, Phys. Rev. Lett. **77**, 3889 (1996).
37. R. J. Schoelkopf et al., Phys. Rev. Lett. **78**, 3370 (1997).
38. P. J. Mohr, B. N. Taylor, J. Phys. Chem. Ref. Data **28**, 1713 (1999).
39. H. Preston-Thomas, Metrologia **27**, 3 (1990).
40. ITS-90 is the international temperature scale of 1990 and PLTS-2000 is the provisional low-temperature scale of 2000.
41. We thank M. Devoret, B. Jarvis, K. Likharev, D. Prober, and W. Tew for useful discussions and the David and Lucile Packard Foundation for support.

Oscillatory Thermomechanical Instability of an Ultrathin Catalyst

Fehmi Cirak,[1] Jaime E. Cisternas,[2] Alberto M. Cuitiño,[5] Gerhard Ertl,[6] Philip Holmes,[2,3] Ioannis G. Kevrekidis,[4,2] Michael Ortiz,[1] Harm Hinrich Rotermund,[6]* Michael Schunack,[6] Janpeter Wolff[6]

Because of the small thermal capacity of ultrathin (~200 nanometers) metal single crystals, it is possible to explore the coupling of catalytic and thermal action at low pressures. We analyzed a chemothermomechanical instability in this regime, in which catalytic reaction kinetics interact with heat transfer and mechanical buckling to create oscillations. These interacting components are separated and explored through experimentation, mathematical modeling, and scientific computation, and an explanation of the phenomenon emerges from their synthesis.

Pattern formation during a surface reaction can be critically affected by temperature changes that are caused by the heat of reaction. Changes in surface temperature locally alter the kinetics of the fundamental processes involved and might lead to ignition and traveling fronts on the active catalyst. Experimental studies of these processes often require tradeoffs: higher gas pressures lead to larger total heat production but also limit the use of surface-sensitive methods for observing fundamental processes.

One way to avoid this tradeoff is to work with ultrathin substrates that have much lower thermal inertia, such as those that have been pioneered by King and co-workers in microcalorimetry studies of surface reactions (1). To study pattern formation during the oxidation of CO on a platinum surface beyond the low-pressure, essentially isothermal regime (2), we used ultrathin (200-nm-thick) Pt(110) single crystals, which should be able to exhibit intense nonisothermal effects for this reaction at intermediate pressures (10^{-2} mbar) (Fig. 1A).

Photoemission electron microscopy (PEEM) images at 4×10^{-4} mbar revealed "raindrop" patterns on the sample, similar to those found before at much higher pressure on a bulk crystal (3), and substantiated their nonisothermal origin. At 5×10^{-3} mbar, where PEEM is not operable, we used a sensitive infrared camera (4), whose main component is a cooled InSb array, capable of imaging temperature differences of

[1]Division of Engineering and Applied Science, California Institute of Technology, Pasadena, CA 91125, USA. [2]Program in Applied and Computational Mathematics, [3]Department of Mechanical and Aerospace Engineering, [4]Department of Chemical Engineering, Princeton University, Princeton, NJ 08544, USA. [5]Department of Mechanical and Aerospace Engineering, Rutgers University, Piscataway, NJ 08854, USA. [6]Fritz-Haber-Institut der Max-Planck-Gesellschaft, Faradayweg 4-6, 14195 Berlin, Germany.

*To whom correspondence should be addressed. E-mail: rotermun@fhi-berlin.mpg.de